



DØnote 4346  
version 1.5

## Measurement of the $t\bar{t} \rightarrow$ all-jets production cross section using Secondary Vertex Tagging

F. Blekman<sup>1</sup> and M. Vreeswijk<sup>1,2</sup>

<sup>1</sup>NIKHEF, Amsterdam, the Netherlands

<sup>2</sup>Universiteit van Amsterdam, Amsterdam, the Netherlands  
(Dated: March 19, 2004)

We have measured the top and anti-top quark ( $t\bar{t}$ ) pair cross section using an event sample corresponding to  $162 \text{ pb}^{-1}$ , which was recorded by DØ in the period 2002/2003. The analysis concentrates on  $t\bar{t}$  pairs decaying in a  $b$ -quark and a  $W$ -boson that decays hadronically. We isolate the  $t\bar{t}$  events from the background using topological variables and a secondary vertex tag (SVT). These variables are combined in a topological analysis which uses artificial neural networks. We observe 220 events with an expected background of  $186 \pm 5(\text{stat}) \pm 12(\text{syst})$  events, with a signal efficiency of  $\epsilon \cdot \text{BR} = 0.0273 \pm 0.0009(\text{stat})_{-0.0079}^{+0.0086}(\text{syst})$ , which corresponds to a cross section of  $\sigma(t\bar{t}) = 7.7 \pm 3.5(\text{stat})_{-1.9}^{+3.7}(\text{syst}) \pm 0.5(\text{lumi})\text{pb}$ .

*Preliminary Results for Winter 2004 Conferences*

## I. INTRODUCTION

This note will describe the analysis method used to do the measurement of the  $t\bar{t} \rightarrow$  all-jets production cross section with a dataset taken between July 2002 and January 2004, with  $\sqrt{s} = 1.96 \text{ GeV}/c^2$ . We use secondary vertex tagging (SVT) for b-jet identification. We do not veto on events with a soft muon tag, but we do reject events that have two or more SVT tagged jets. First, we will discuss the parametrization of the QCD background with tag rate functions (TRF), after which we will continue with the kinematic variables, which are then used in a chain of top-discriminating neural networks. We will shortly discuss the neural network training, after which we use the neural networks to predict the number of observed signal and background events.

## II. DATASET

We use the dataset, signal Monte Carlo and kinematic variables as described in detail in DØ note 4333[1]. Our dataset consists of almost 300k 6-jet events, and measured to contain an integrated luminosity of  $162 \text{ pb}^{-1}$  at an average trigger efficiency of 77% after preselection. This number is derived by parametrization of the physics objects (=jets) in the event, and is described in detail in [3, 4]. Correction for the trigger efficiency is done on event basis, and is included in all distributions in this note. Our data and all our Monte Carlo samples are processed with the *Nefertiti* version of top\_analyze.

## III. MODELING QCD BACKGROUND USING TAG-RATE FUNCTIONS

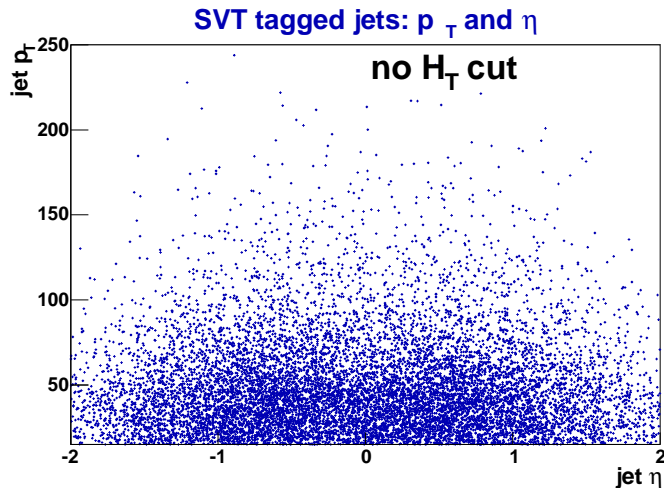


FIG. 1: SVT tagged jets:  $\eta$  versus  $p_T$ .

The presence of two b-jets in  $t\bar{t}$  events leads to relatively high yield of SVT tagged jets.

The overwhelming presence of QCD events in the tagged (and untagged) sample allows to measure the SVT tag rate function (TRF) in a straightforward manner. The TRF gives us the probability to tag a random (background) event in our sample. We measure the TRF

on a jet by jet basis and calculate the probability, that a QCD event contains exactly one tagged jet:

$$P(\text{tags} = 1) = \sum_i p_i \prod_{j \neq i} (1 - p_j).$$

To first order, the TRF is modeled as function of the transverse energy and rapidity of the jets. If there are no large  $\eta$  and  $p_T$  correlations (Figure 1), the tag rate function factorizes:

$$P_{tag}^{jet}(p_T, \eta) = N f(p_T) g(\eta). \quad (1)$$

with  $f(p_T)$  the probability that a jet with transverse energy has a SVT tag,  $g(\eta)$  the probability that a jet at  $\eta$  is tagged and  $N$  a normalization factor, which is needed to make sure the integral of the total tagging probability is normalized to unity.

Similar to all other track-based b-tag analyses in the top group, we use physics  $\eta$ , not detector  $\eta$  for the parametrization.

We correct the jet  $p_T$  with the light quark jet energy scale. As we apply our TRF to tagged and untagged events, and the probability for a tagged event to contain a muon is higher, we would shift our signal  $p_T$  distribution more than our background  $p_T$  distribution if the jet energy scale were corrected for the missing momentum from the neutrino. We want to be able to compare our tagged and untagged jets and events, as our tagged sample is also expected to be mainly background. Hence, we do not apply the muon jet energy scale for jets that contain a (soft) muon.

Figure 2 shows ratio of tagged jets over all taggable jets,

$$TRF = \frac{N_{tagged}(p_T, \eta, H_T)}{N_{taggable}(p_T, \eta, H_T)},$$

as function of the jet  $p_T$ . We use the same definition of taggability as all other lifetime tagging  $t\bar{t}$  analyses[5]: The jet needs to contain at least two tracks ( $p_T > 0.5$  GeV and  $\chi^2 < 3$ ) within a  $\Delta R(\text{track}, \text{jet}) < 0.5$ , where each track should have at least three SMT hits or at least two hits in the two inner layers of the silicon. When using the TRF for our background predictions, we only apply our TRF to taggable jets. The function  $f(p_T)$  (also shown) is fitted to ratio of these distributions, using a parametrization of the form:

$$f(p_T) = a_0 \cdot 0.5(1 + \text{Erf}(frac{p_T - a_1 a_2 \sqrt{p_T}})),$$

where Erf is the standard gaussian error function. The function  $g(\eta)$  is obtained in a similar manner and is parametrized as:

$$g(\eta) = b_1 + b_2 \eta^2 + b_3 \eta^4 + b_4 \eta^6 + b_5 \eta^8 \quad (2)$$

As this is an even function, we implicitly make the presumption that the behavior of SVT is relatively symmetric in  $\eta$ .

The rate of SVT tagged jets as function of  $\eta$  and the fitted function  $g(\eta)$  is displayed in Fig 3. The normalization factor  $N$  is fixed by the requirement:

$$N_{tagged}^{jets} = \sum_{jets} N f(p_T) g(\eta). \quad (3)$$

The  $p_T$  and  $\eta$  distribution of the tagged jets, together with the expected number of tagged jets are shown in figure 5.

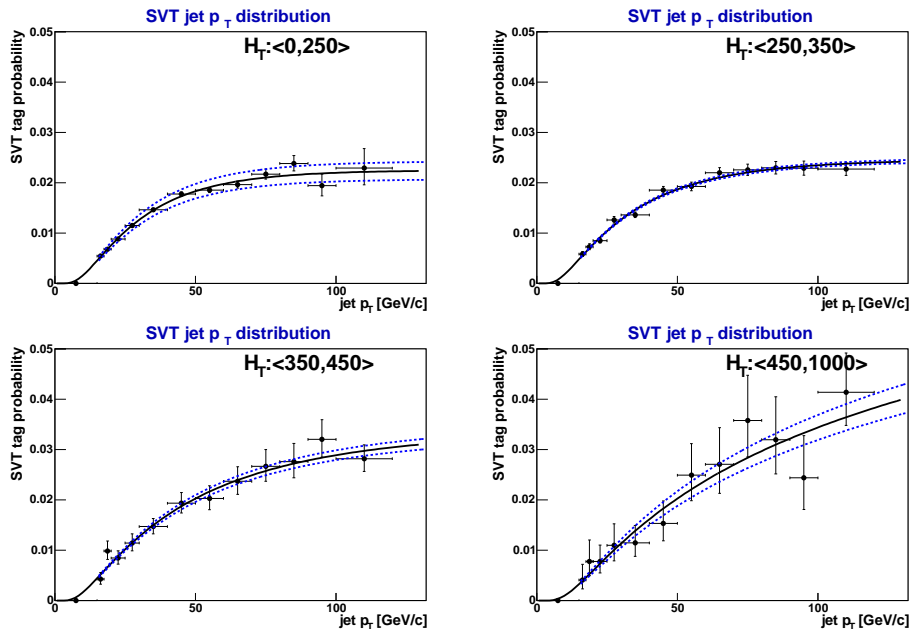


FIG. 2: The behavior of  $f(p_T)$  for different  $H_T$  bins.

We observe that there is a  $H_T$ -dependence of the shape of the turn-on function. Figure 2 shows the behavior of  $f(p_T)$  for different  $H_T$  bins.

We also observe that, even after the correction for the changes in turn-on of  $f(p_T)$ , the number of jets tagged  $N_{tagged}^{jets}$  is linearly dependent of the transverse energy in the event,  $H_T$  (Figure 4).

The expected number of jets now becomes:

$$N_{tagged}^{jets} = N(H_T) \sum_{jets} f(p_T)g(\eta).$$

### A. Background prediction using TRFs

On jet level, we can confirm the performance of our TRF as a function of jet pseudo-rapidity and transverse momentum, as the distribution is produced directly by weighing the untagged data with the jet weights. Figure 5 shows that the prediction is in rather good agreement, both when the TRF is applied to each jet separately, and when applied to the event as a whole.

### B. Quality of TRF prediction on event basis

The TRF is used to predict the probability that a background event will have a SVT tag. We do not care if this tag is real or a mis-tagged light quark jet.

We have observed that the TRF prediction is almost not dependent of the topological part of the analysis, the variables *Aplanarity*, *Sphericity*, *Centrality* and  $\langle \hat{\eta}^2 \rangle$ . On

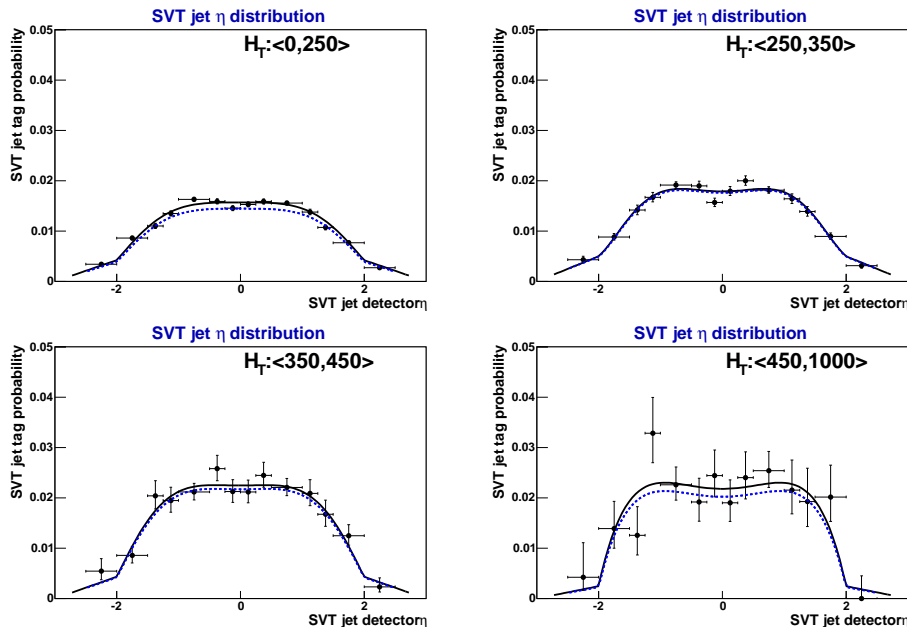


FIG. 3: The behavior of  $g(\eta)$  for different  $H_T$  bins.

the other hand, the background prediction is very dependent on the energy-dependent variables like  $H_T$ . To study this effect, we train a dedicated neural network  $nn_{QCD}$ , which has *Aplanarity*, *Sphericity*, *Centrality* and  $\langle \hat{\eta}^2 \rangle$  as input variables. This neural net is used instead of one of the topological variables because it gives us a better control on rejection of our potential top content in our TRF.

To parametrize the background-content of our sample, we want to make sure that our background dominated region is absolutely normalized. For this, we apply our TRF to all events and look at the behavior of the output of  $nn_{QCD}$ . The result of this procedure is shown in 6. Figure 7 gives us the scatter of the normalization of  $nn_{QCD}$ . Our expected background region is in the region  $nn_{QCD} < 0.6$ , while even in the higher regions we do not expect a dominant excess of top events. We use all events with  $nn_{QCD} < 0.6$  to get an estimate on the error of our background estimation method. As figure 7 shows, we need to apply a scale factor of 4% if we only want to use background events to predict the background-content in our tagged sample. The error from this procedure is used as a systematic uncertainty on the analysis, and is also shown in all following kinematic distributions as an error on the background prediction. Table I shows the quality of the TRF prediction when the error on the scale factor is already taken into account, and shows that our used error of 7% can be considered conservative.

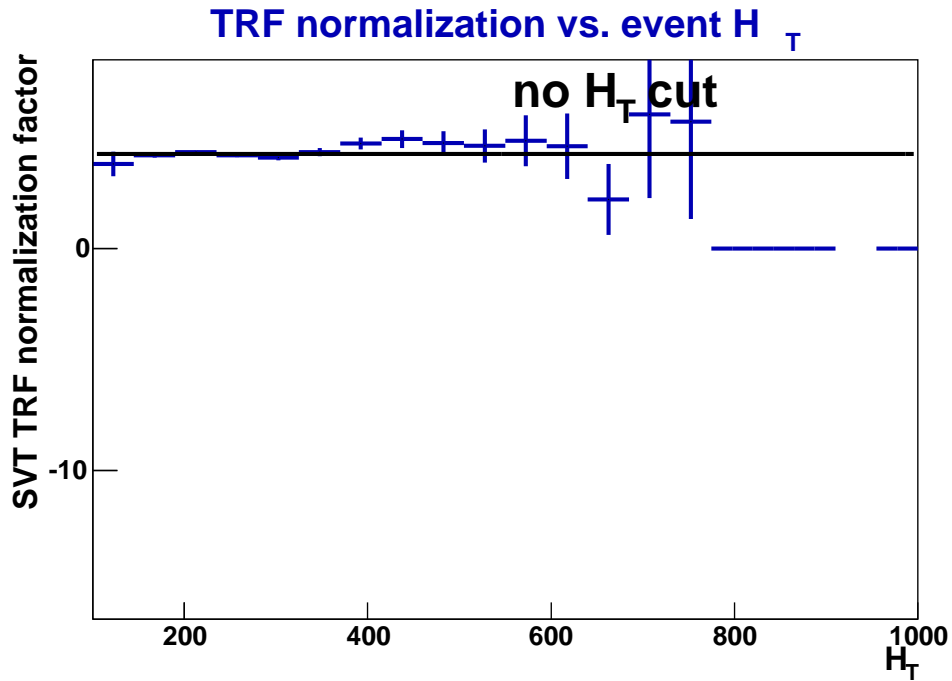


FIG. 4: The probability to tag a jet is dependent of all the transverse energy in the event,  $H_T$ . We parametrize this behaviour by the fitted line shown, which is used to normalize our background parametrization.

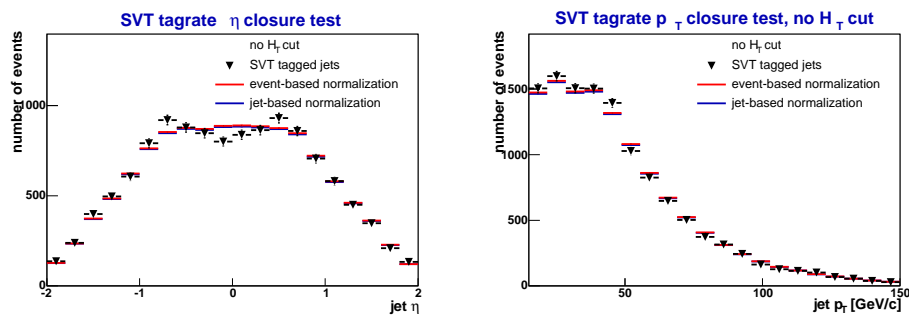


FIG. 5: TRF prediction of the number of tagged jets vs.  $\eta$  (left) and  $p_T$  (right).

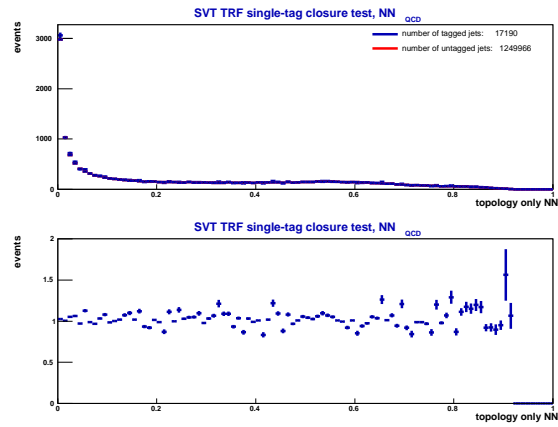


FIG. 6: *Top*: Number of observed and predicted events for different bins in  $nn_{QCD}$ . *Bottom*: ratio between the number of observed and predicted events, should be a horizontal line around ratio=1.

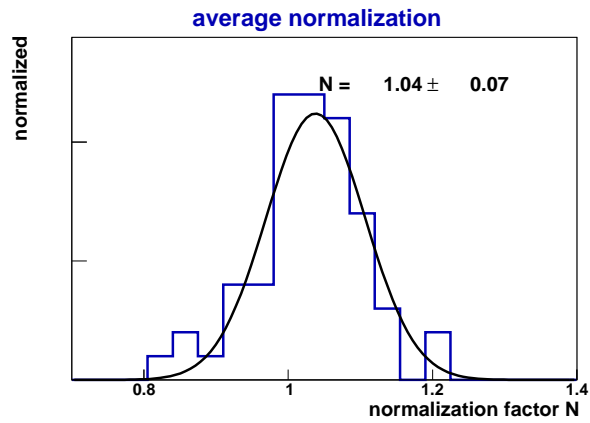


FIG. 7: *The scale factor needed to apply our event-weight*

Variable	Statistical errors only		including systematic errors	
	$\chi^2/N_{DF}$	Probability of $\chi^2$	$\chi^2/N_{DF}$	Probability of $\chi^2$
$H_T$	3.91871 / 14	0.995936	2.61665 / 14	0.999581
$\sqrt{s}$	14.4999 / 20	0.804272	9.89883 / 20	0.969969
$H_T^{3j}$	12.9779 / 16	0.674373	5.55592 / 16	0.992222
$E_{T_{5,6}}$	10.2135 / 12	0.597239	2.70008 / 12	0.997316
$N_{jets}^A$	10.4086 / 11	0.494052	5.03841 / 11	0.929292
Aplanarity	25.7636 / 19	0.135911	11.3802 / 19	0.910384
Sphericity	31.5477 / 24	0.138611	15.1633 / 24	0.915889
Centrality	17.8932 / 18	0.462706	8.25709 / 18	0.974559
$\langle \eta^2 \rangle$	14.0729 / 19	0.779427	7.02727 / 19	0.994066
Mass Likelihood ( $t\bar{t}$ )	26.5909 / 31	0.692556	19.6284 / 31	0.943439
Mass Likelihood ( $W$ )	31.7399 / 31	0.429419	20.7496 / 31	0.918359
$M_{12}^{min}$	17.4906 / 18	0.489652	9.0867 / 18	0.9577
$M_{34}^{min}$	23.4586 / 21	0.320021	12.8136 / 21	0.915013
$NN0$	41.4639 / 30	0.0794822	21.0275 / 30	0.887025
$NN_{QCD}$	28.1424 / 28	0.45692	14.6379 / 28	0.982009

TABLE I:  $\chi^2 = (N_{obs} - N_{pred})^2 / (\sigma_{obs}^2 + \sigma_{pred}^2)$  per degrees of freedom for all topological variables and the lower-level neural nets. The used errors include the statistical error on the tagged events, and respectively only the statistical or the statistical and and systematic error (from TRF normalization) added in quadrature for the background prediction. Bins containing less than 10 tagged events are not used in the calculation. The actual distributions will be shown in section IV.

#### IV. KINEMATIC VARIABLES

The kinematic variables used in this analysis are identical to the ones described in DØnote 4333[1]. The background event distributions are created by multiplying all events by the probability to tag an event in our sample  $p_{bg}(p_T, \eta, H_T)$ .

All figures contain the distributions for events with one SVX tag, the background prediction and its errors (from limited statistics and the error on the TRF), and the expected distribution for top events, weighed with the per-event trigger efficiency. The  $t\bar{t}$  contribution is normalized to the number of tagged events, and is only added to provide extra information on the difference between QCD 6-jet events and signal 6-jet events.

For each topological variable, we also show the quality of the background prediction,

$$\frac{N_{predicted} - N_{observed}}{N_{predicted}},$$

where all statistical errors and the systematic error on the trf are propagated to the distribution.

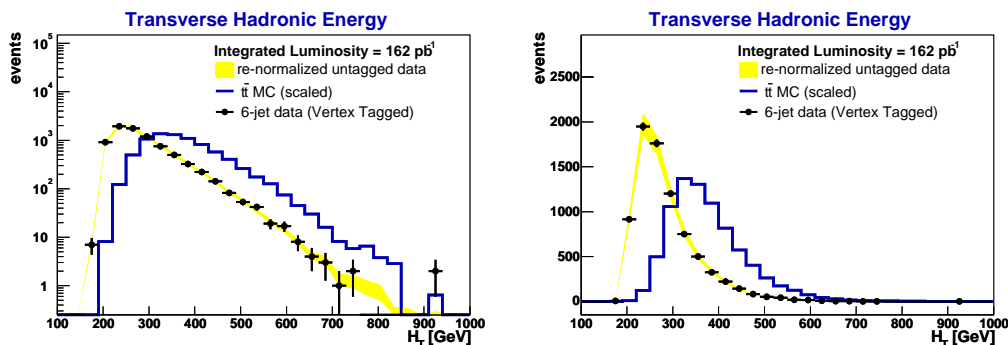


FIG. 8:  $H_T$  distribution for Monte Carlo (filled histogram), SVT tagged events (markers) and predicted background (error band).

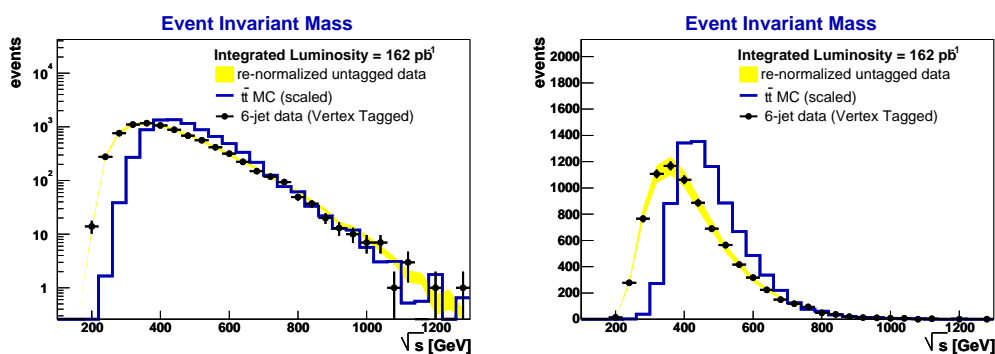


FIG. 9:  $\sqrt{s}$  distribution for Monte Carlo (filled histogram), SVT tagged events (markers) and predicted background (error band).

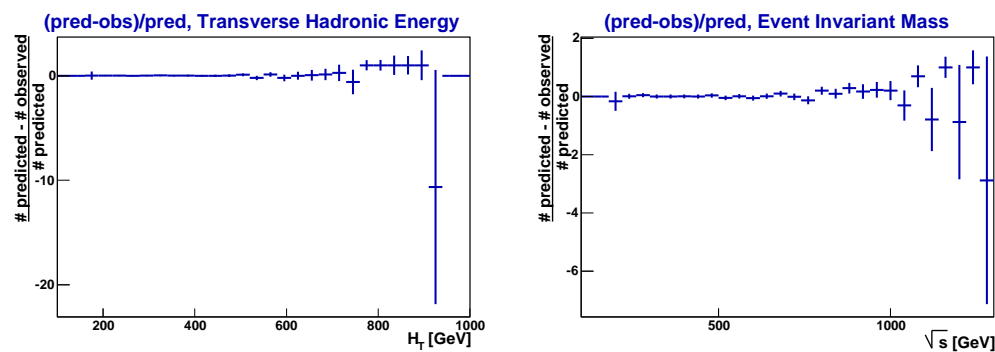


FIG. 10:  $\frac{N_{pred} - N_{obs}}{N_{pred}}$  for  $H_T$  (left) and  $\sqrt{s}$  (right).

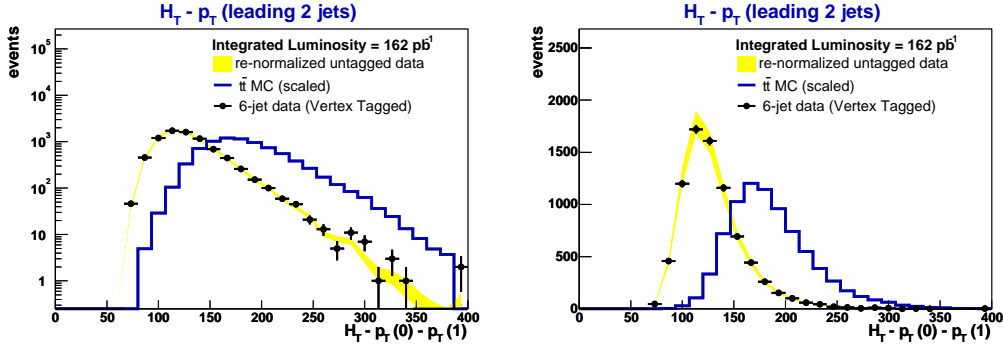


FIG. 11:  $H_T^{3j}$  distribution for Monte Carlo (filled histogram), SVT tagged events (markers) and predicted background (error band).

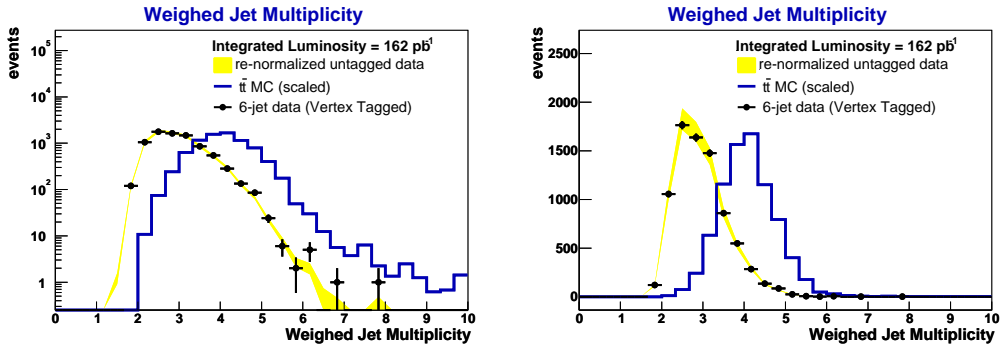


FIG. 12:  $N_{jets}^A$  distribution for Monte Carlo (filled histogram), SVT tagged events (markers) and predicted background (error band).

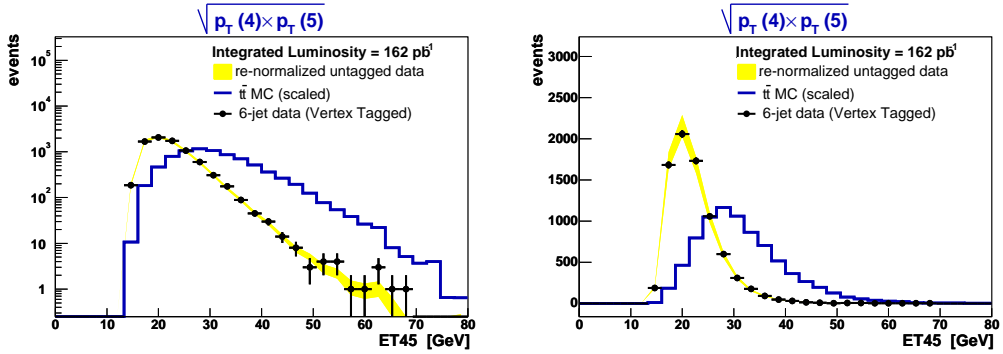


FIG. 13:  $E_{T_{5,6}} = \sqrt{E_T(jet5) \cdot E_T(jet6)}$  distribution for Monte Carlo (filled histogram), SVT tagged events (markers) and predicted background (error band).

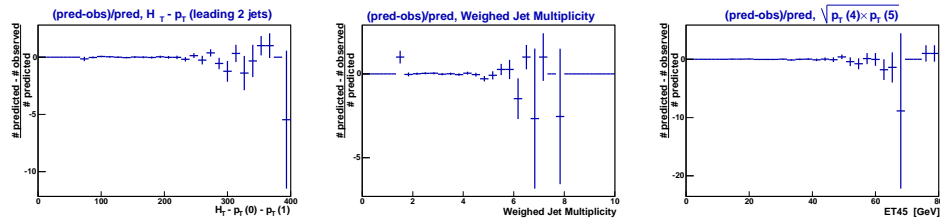


FIG. 14:  $\frac{N_{pred} - N_{obs}}{N_{pred}}$  for  $H_T^{3j}$  (left),  $N_{jets}^A$  (center) and  $E_{T_{5,6}}$  (right).

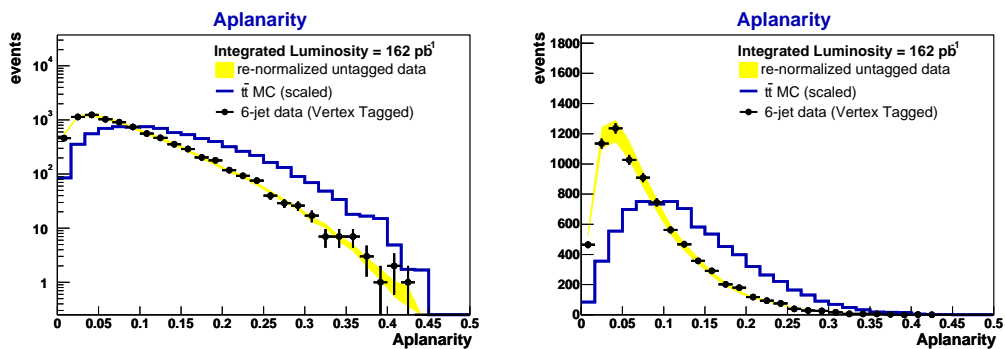


FIG. 15: Aplanarity distribution for Monte Carlo (filled histogram), SVT tagged events(markers) and predicted background(error band).

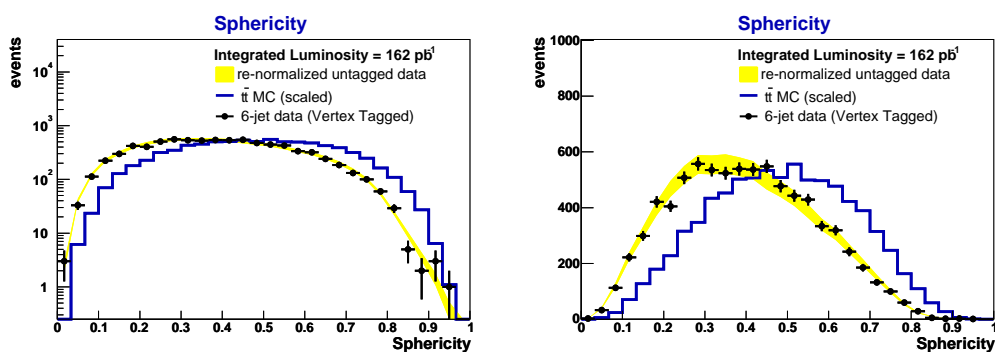


FIG. 16: Sphericity distribution for Monte Carlo (filled histogram), SVT tagged events(markers) and predicted background(error band).

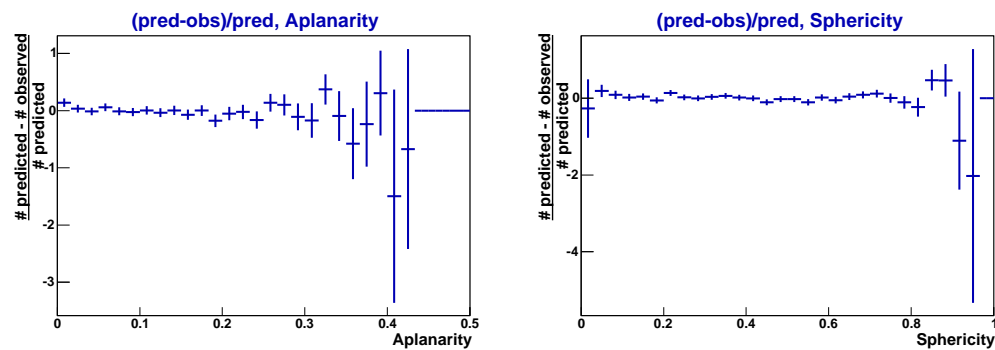


FIG. 17:  $\frac{N_{pred} - N_{obs}}{N_{pred}}$  for aplanarity(left) and sphericity(right).

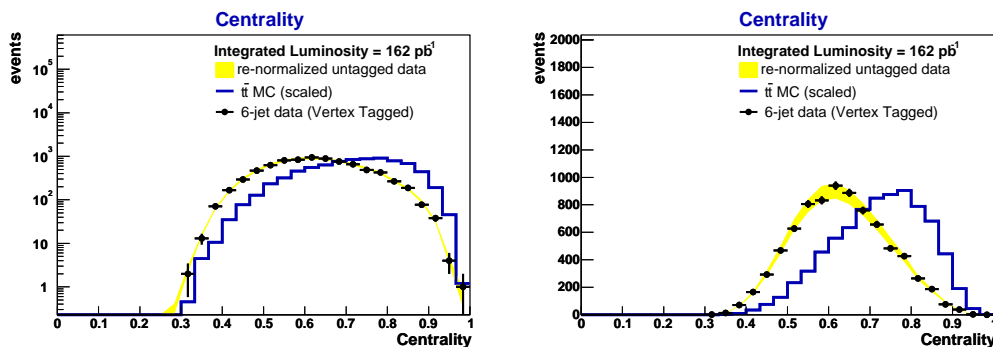


FIG. 18: Centrality distribution for Monte Carlo (filled histogram), SVT tagged events (markers) and predicted background (error band).

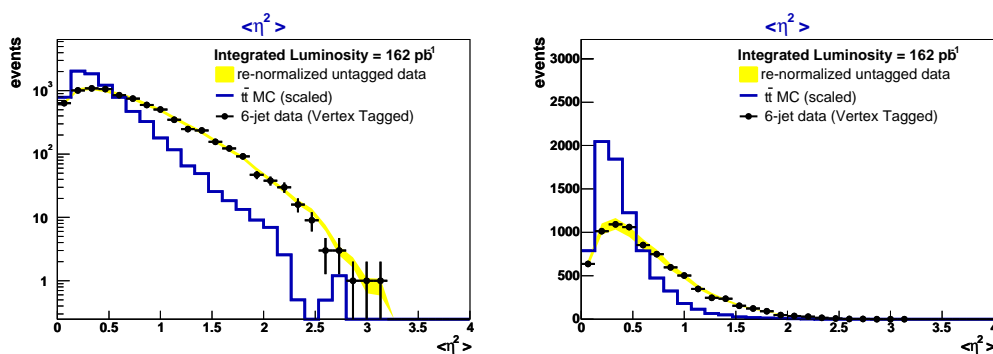


FIG. 19:  $\langle \eta^2 \rangle$  distribution for Monte Carlo (filled histogram), SVT tagged events (markers) and predicted background (error band).

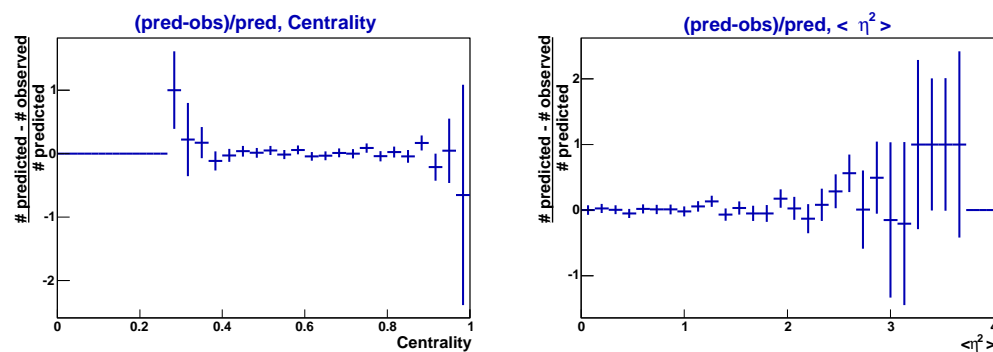


FIG. 20:  $\frac{N_{pred} - N_{obs}}{N_{pred}}$  for centrality (left) and  $\langle \eta^2 \rangle$  (right).

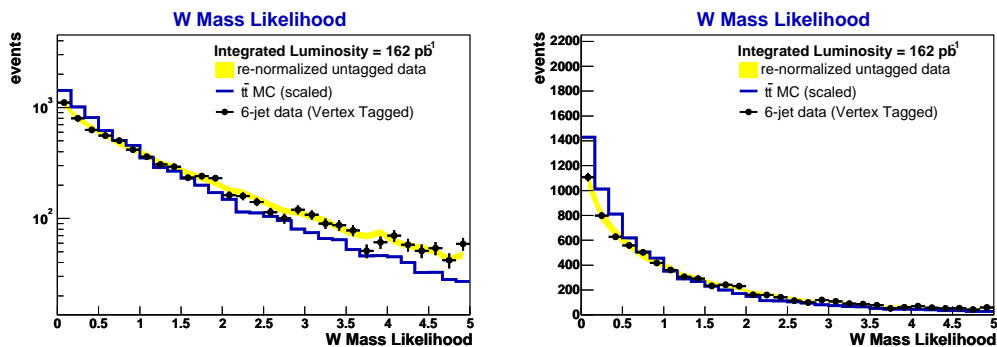


FIG. 21:  $W$  mass likelihood distribution for Monte Carlo (filled histogram), SVT tagged events (markers) and predicted background (error band).

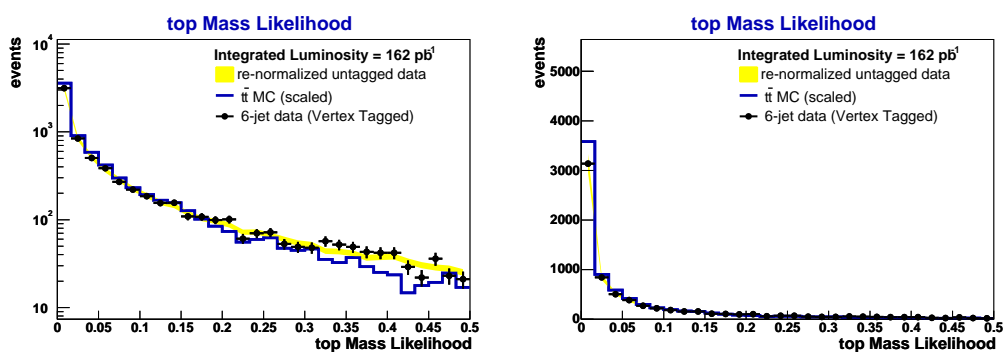


FIG. 22: Top mass likelihood distribution for Monte Carlo (filled histogram), SVT tagged events (markers) and predicted background (error band).

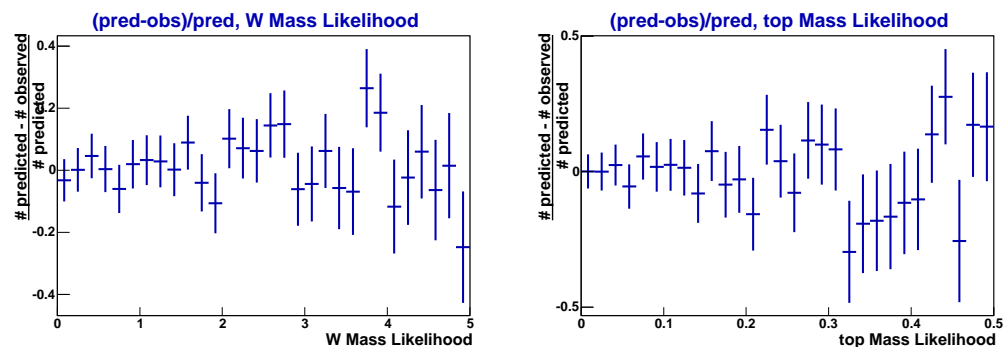


FIG. 23:  $\frac{N_{pred} - N_{obs}}{N_{pred}}$  for  $W$  mass likelihood (left) and  $t$  mass likelihood (right).

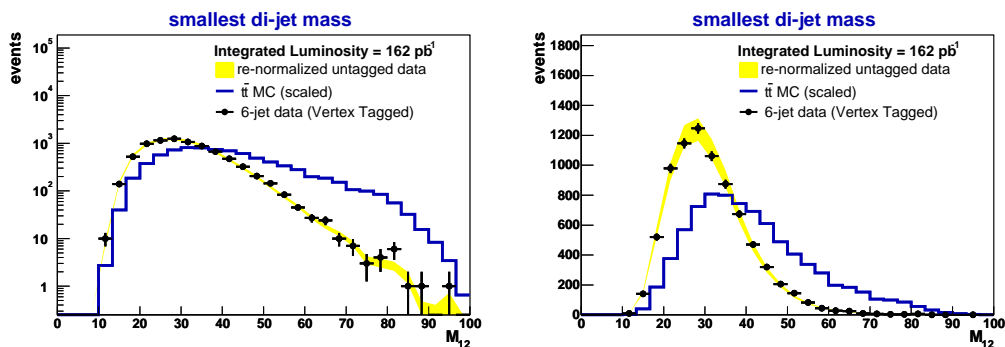


FIG. 24:  $M_{12}^{min}$  distribution for Monte Carlo (filled histogram), SVT tagged events (markers) and predicted background (error band).

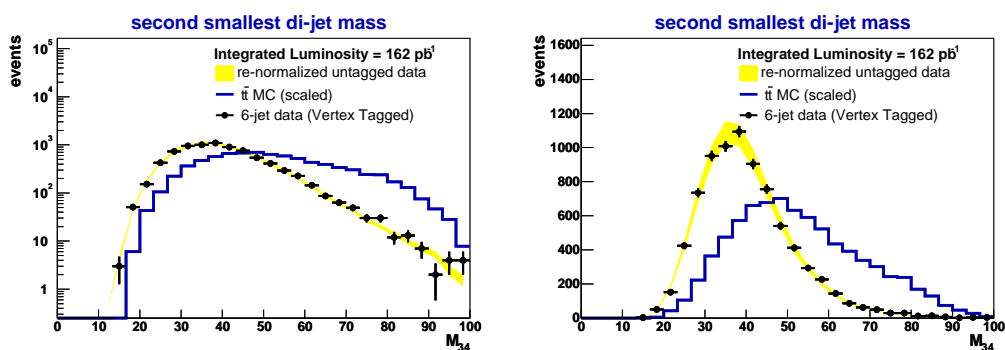


FIG. 25:  $M_{34}^{min}$  distribution for Monte Carlo (filled histogram), SVT tagged events (markers) and predicted background (error band).

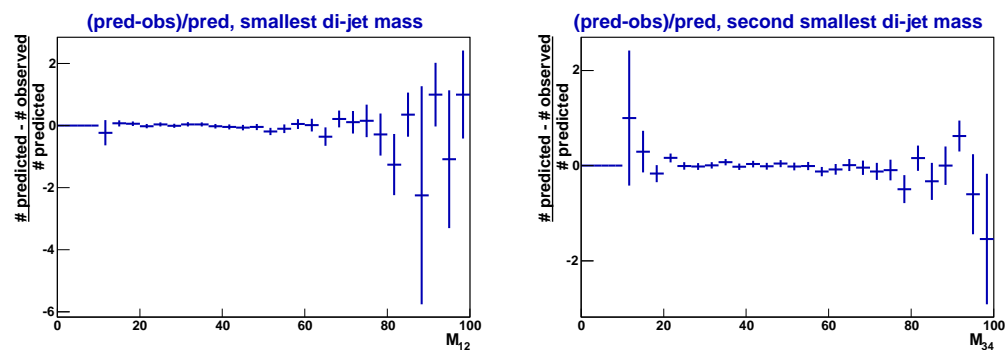


FIG. 26:  $\frac{N_{pred} - N_{obs}}{N_{pred}}$  for  $M_{12}^{min}$  (left) and  $M_{34}^{min}$  (right).

## V. NEURAL NETWORKS

We combine the quantities introduced above utilizing a chain of (artificial) neural networks (NNs). NNs provide the best possible discriminating power by accounting for the correlations between their input variables. We use feed-forward NNs, trained by back propagation as implemented in the JETNET[6] program. All the NNs have 1 output node and 1 middle layer with a number of nodes, twice the number of the input layer.

### A. training samples

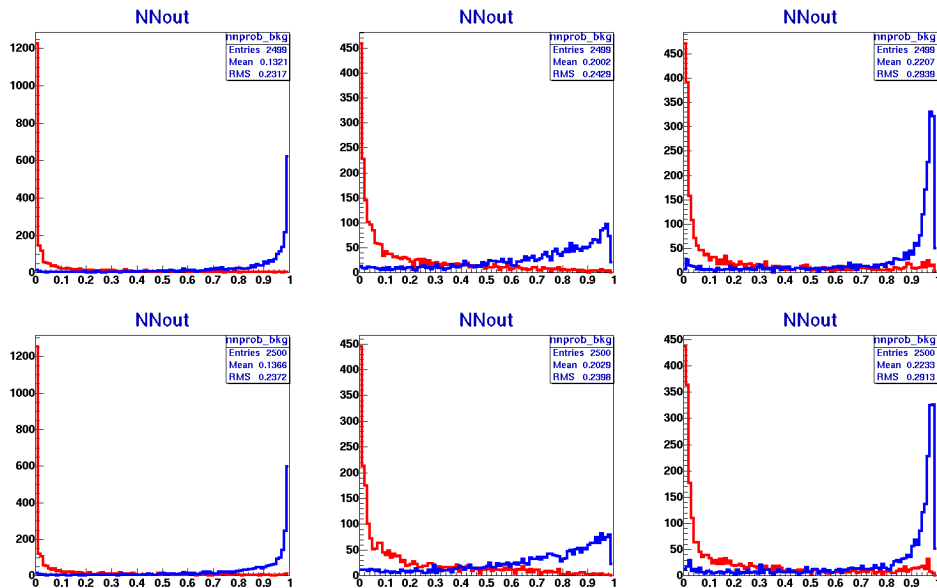


FIG. 27: Neural network training output distributions for NN0 (left), NN1 (center) and NN2 (right). The top plots give the NN output for the training sample, the bottom plots show the distributions for an identically selected (but different) sample of the same size.

The NNs are trained on a small, randomly chosen fraction (5000 events,  $\approx 3\%$ ) of our background sample and MC simulated  $t\bar{t}$  events. The random selection is done as follows:

- Random selection: We draw a random event from our event sample.
- Tagged events rejection: We reject events with a soft muon or SVX tag. For Monte Carlo we do not reject tagged events, but we also do not use the tagging information.
- Weighed random event rejection: We draw a random number from a uniform distribution between 0 and 1. If our event tagging probability is higher than this random value, we use the event. For Monte Carlo simulated events we require the event tagging probability times the trigger efficiency to be higher than the random value. This method is based on the idea that we want our NNs to be trained on events which have a high chance of having a tag, without actually using tagged events in the training.
- We continue this process until we have 5000 training events.

- The first 2500 training events are used for training, the second 2500 are used for cross-checking the neural network output. Figure 27 shows the output distributions for the training sample for the three neural networks.

Note again that data events containing a soft muon or SVX tag are never used in the training of the NNs. The neural network discriminant output for the complete training samples can be seen in figure 27.

## B. Pre-selection with NN0

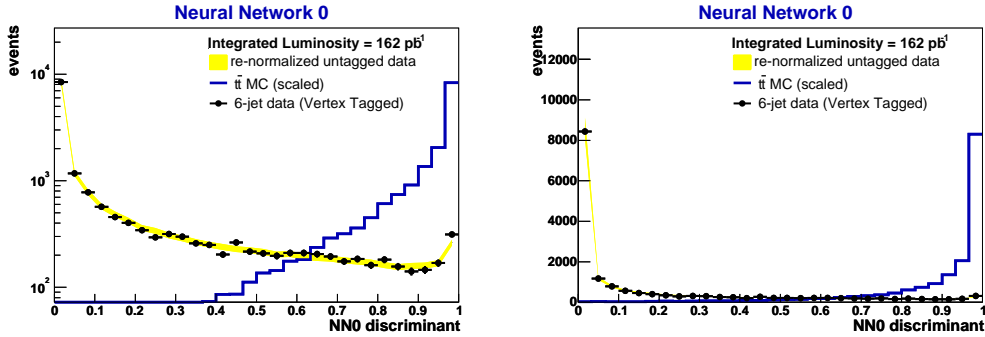


FIG. 28:  $NN0$  distribution for tagged (markers) and untagged (error band) data, and for signal Monte Carlo. Events with  $NN0$  discriminant  $< 0.05$  are removed from the further analysis.

The data is first pre-selected using a neural network ( $NN0$ ), which has as input  $H_T$ ,  $\sqrt{s}$ ,  $H_T^{3j}$ ,  $N_{jets}^A$ , *sphericity*, *aplanarity* and *centrality*. As this pre-selection only removes events that are very obvious background, this enhances the sensitivity for  $t\bar{t}$  signal of our analysis. The output distribution of  $NN0$  can be seen in figure 28.

To reduce the number of background events in the final distribution, we make cuts on the discriminant of the output of the first neural network:

$$NN0 > 0.05 \quad (4)$$

Events which fail this cut are rejected from the further analysis, and are also not used for neural network training purposes. Our sample is still background-dominated after the  $NN0 > 0.05$  requirement. The efficiencies of this cut for data and Monte Carlo simulated events can be seen in table II.

## C. Selection with NN1

After the pre-selection with  $NN0$  we use  $NN1$  to provide a single discriminant.  $NN1$  takes as input variables  $H_T$ ,  $\sqrt{s}$ ,  $E_T(\text{jet1})/H_T$ ,  $H_T^{3j}$ ,  $N_{jets}^A$ ,  $E_T^{5,6}$ , *sphericity*, *aplanarity*, *centrality* and  $\langle \eta^2 \rangle$ . The output of  $NN1$  is used as an input variable of  $NN2$ . The output of  $NN1$  for background (including error on background) and signal data can be seen in figure 29.

The use of two neural networks instead of one is mainly based on the fact that the analysis presented in this note is heavily based on the Run I analysis. Another reason is

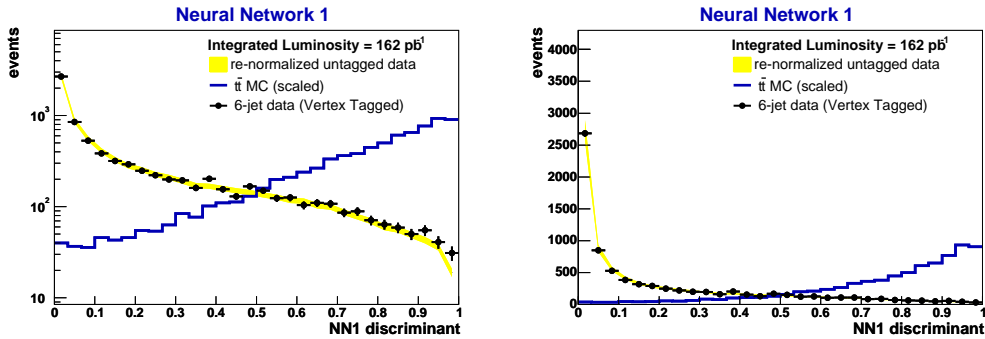


FIG. 29:  $NN1$  distribution for tagged (markers) and untagged (error band) data, and for signal Monte Carlo. Events with  $NN1$  discriminant  $< 0.05$  are removed from the further analysis.

that in principle it is much easier to include some b-tagging information in neural network 2, because there should be no change in the kinematic distributions when b-quark identification is applied. The turn-on of the tagging efficiency versus the jet  $p_T$  if corrected for by the tag rate functions.

#### D. Second Neural Network

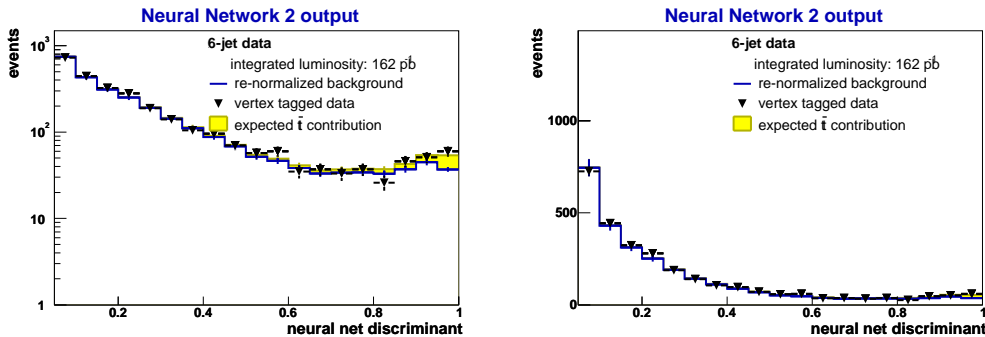


FIG. 30:  $NN2$  distribution for tagged events (markers), expected background only (open histogram) and expected signal+background (filled histogram). We presume the production cross section to be  $7 \text{ pb}^{-1}$ ,  $BR(\text{all-jets})=0.46$  and the top mass to be  $175 \text{ GeV}/c^2$ .

The final NN,  $NN2$ , takes as input the output of  $NN1$  and the the mass likelihoods  $\mathcal{M}_{t\bar{t}}$  and  $\mathcal{M}_{WW}$ , and the smallest di-jet masses  $M_{min}^{1,2}$  and  $M_{min}^{3,4}$ .

Figure 30 shows the expected distributions presuming a  $t\bar{t}$  cross section of  $8 \text{ pb}^{-1}$ . In the tagged sample the  $t\bar{t}$  signal is still expected to be around one order of magnitude smaller than the background.

efficiencies				
	tt $\rightarrow$ all - jets		tt $\rightarrow$ lepton + jets	
	marginal	cumulative	marginal	cumulative
pre-selection	$0.3884 \pm 0.0029$	$0.3884 \pm 0.0029$	$0.0375 \pm 0.0009$	$0.0375 \pm 0.0009$
trigger	$0.7367 \pm 0.0080$	$0.2861 \pm 0.0023$	$0.4982 \pm 0.0191$	$0.0187 \pm 0.0006$
$NN0 > 0.05$	$0.9968 \pm 0.0113$	$0.2852 \pm 0.0023$	$0.9830 \pm 0.0418$	$0.0183 \pm 0.0006$
$N_{SVT} = 1$	$0.457549 \pm 0.0051608$	$0.130502 \pm 0.00103148$	$0.481087 \pm 0.0203224$	$0.00882647 \pm 0.000260199$
$NN2 > 0.75$	$0.456203 \pm 0.00666659$	$0.0595354 \pm 0.000731762$	$0.220211 \pm 0.0166007$	$0.00194369 \pm 0.000134858$

TABLE II: *Efficiencies and number of observed events for all analysis cuts.*

## VI. CROSS SECTION MEASUREMENT

In this section we present our results for the measured number of events in the  $t\bar{t}$  all-jets channel. The measurement is based on the output of neural network  $NN2$  for the signal sample (SVX tagged events). The number of events above a threshold on the output of  $NN2$  are counted. The remaining background is predicted from untagged events, weighted with a muon tag rate function.

The expected  $NN2$  distribution, and the prediction of the distribution when only background is expected, can be seen in figure 31.

### A. Signal tagging probability

We use the certified  $b/c/q$ -tagging probabilities for data supplied to us by the DØ b-ID group. We use the probability that an event has exactly one tag, and use this probability as a weighing factor for our signal Monte Carlo.

	$P_{tag} t\bar{t}$	
	direct MC tagging	parameter tagging
$b$ -jets	0.52	0.39
$c$ -jet	0.13	0.11
light $q$ -jet	0.003	0.006

TABLE III: *The probability to tag jets of different flavor, for our Monte Carlo sample after pre-selection, and our (data-based) SVT tag parametrization*

The probability for jet in a  $t\bar{t} \rightarrow$  all-jets event to have a tag depends on the flavor of the jet, and is listed in table III.

### B. Cross section using counting method

The tag rate functions are applied to full sample (only double-tags excluded) to estimate the number of background events in our tagged sample. The excess number of events above a certain  $NN2$  discriminant, together with the efficiency for signal for this cut, is used to calculate the  $t\bar{t}$  cross section. The optimal value of the cut on  $NN2$  can be determined by

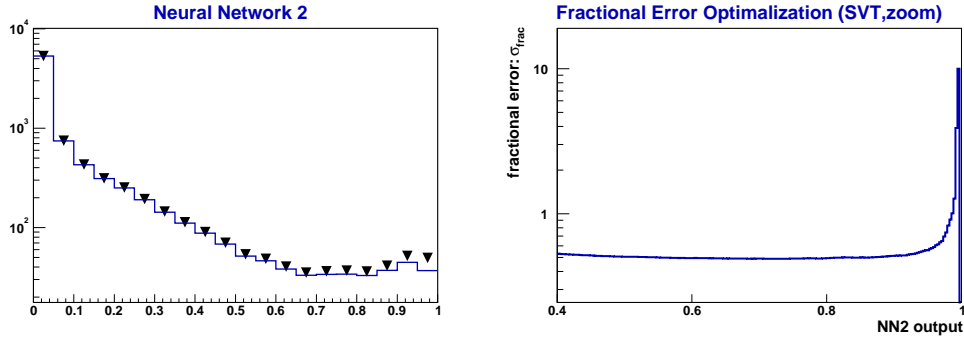


FIG. 31: *Left: NN2 output distribution for expected background (histogram) and expected signal+background (triangles). Trigger efficiency and SVX tagging efficiencies from data are already taken into account. Right: NN2 output fractional error for different NN2 discriminant cuts. The minimal fractional error value is minimal at NN2  $\simeq$  0.75 .*

minimizing the expected signal fractional error. This property is:

$$\sigma_{frac}(NN2 \text{ cut}) = \frac{\sqrt{s_{exp} + b_{exp}}}{s_{exp}}, \quad (5)$$

where  $s_{exp}$  and  $b_{exp}$  respectively represent the number of expected signal and expected background events which have  $NN2$  values above a certain threshold.

Figure 31 shows the expected number of background events, together with the total number of expected events, i.e. signal+background. As can be seen in figure 31,  $\sigma_{frac}$  is minimal at a  $NN2$  cut of 0.75. When this cut of  $NN2 > 0.75$  is applied, we observe the following numbers of events:

$$N_{background}(\text{expected}) = 186 \pm 5 \text{ events},$$

where the error comes from statistical fluctuations in our background distribution only. In the single-tagged sample, we observe the following:

$$N_{observed} = 220 \text{ events} \quad (6)$$

Figure 32 shows the observed  $NN2$  distribution, together with the distributions that would be expected if only background or background and  $t\bar{t} \rightarrow$  all-jets signal were present in the dataset.

The efficiency for the selected cut is measured on  $t\bar{t} \rightarrow$  alljets Monte Carlo simulated events, which are already corrected for the efficiency of the trigger and the probability to have one SVX tag:

$$\epsilon_{\text{all-jets}} = 0.058 \pm 0.0007(\text{stat}),$$

where the statistical errors are due to our Monte-Carlo statistics. This efficiency still has to be corrected for events from the other  $t\bar{t}$  production channels, especially the  $\tau$ +jets channel can be expected to have an event topology that is similar to the fully hadronic top decays:

$$\epsilon_{\text{lepton+jets}} = 0.0018 \pm 0.0001(\text{stat}). \quad (7)$$

The influence of the different selection criteria on the analysis efficiency is listed in table II. Combining these two efficiencies according to the expected branching ratios (which are,

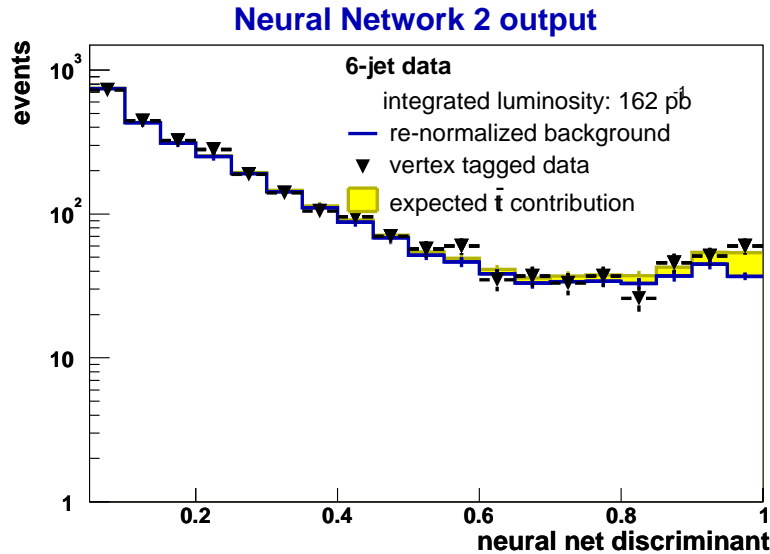


FIG. 32: NN2 output distribution for muon-tagged events (triangles), expected background (open histogram) and expected signal+background (filled histogram)

respectively,  $0.460 \pm 0.014$  for the all-jets and  $0.437 \pm 0.007$  for all three lepton+jets channels combined) gives us an efficiency to measure the cross section for all  $t\bar{t}$  production channels which produce an event topology of at least 6 jets and no isolated leptons. This gives us a final signal efficiency of

$$\epsilon \cdot \text{BR} = 0.0273 \pm 0.0009(\text{MC}, \text{BR}),$$

where the error includes the errors on the PDG values for the all-jets and lepton+jets branching fractions. The cross section is defined as

$$\sigma = \frac{N_{\text{observed}} - N_{\text{background}}}{\mathcal{L} \cdot \text{BR} \cdot \epsilon(t\bar{t})} \quad (8)$$

where  $\mathcal{L}$  is the presumed luminosity of the dataset used. The luminosity was measured to be  $\mathcal{L} = 162 \pm 6.5\% \text{pb}^{-1}$ . Using this value, together with the observed events (VIB), (6) and efficiency(VIB), we measure the cross section to be:

$$\sigma(t\bar{t}) = 7.7 \pm 3.5(\text{stat}) \text{ pb} \quad (9)$$

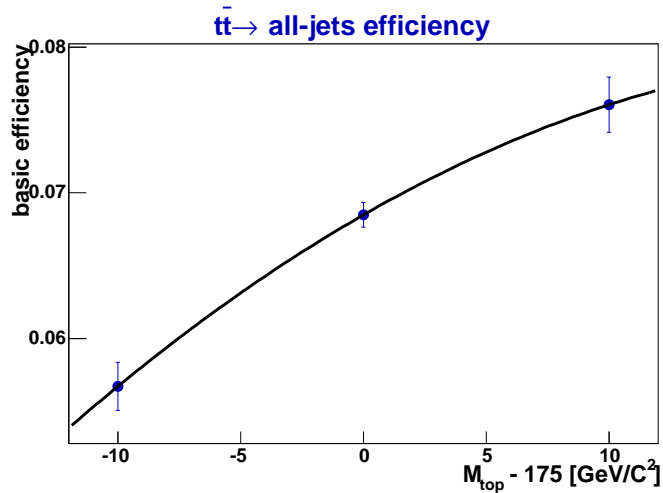


FIG. 33: Signal efficiency dependence of the top mass. We use the values at  $-5$  and  $+5$   $\text{GeV}/c^2$ .

## VII. SYSTEMATIC UNCERTAINTIES

We include the following systematic effects in our systematic error calculation. The actual errors are listed in tables IV and VI for errors that influence the efficiency and excess, respectively.

- The error on the measurement of the vertex reconstruction
- The influence of the difference in jet ID between Monte Carlo simulation and data. The current jet identification uses a first-level trigger confirmation in its selection criteria. We overcompensate for this effect by making a (conservative) parametrization of the probability that a jet will not be reconstructed. We use a dedicated version of the top tuple maker `top_analyze` for this purpose.
- The influence of the error on the jet energy scale. We use the standard procedure of varying the applied JES by adding (subtracting) the quadratic sum of the systematic and statistical uncertainty for data and Monte Carlo jets by one sigma.
- The influence of the Monte Carlo smearing of the jet energy resolutions. We have a dedicated version of `top_analyze` that over(under) smears the jet energies on our signal Monte Carlo.
- The analysis efficiency is dependent on the top mass that was used. We calculate the efficiency for a top mass of  $175 \text{ GeV}/c^2$ , and have control samples at  $165$  and  $185 \text{ GeV}/c^2$ . We obtain the error on a variance of  $\pm 5 \text{ GeV}/c^2$  (the world average error) through interpolation, as is shown in figure 33.
- The uncertainty on the trigger parametrizations. We assume this to be 4%, which is the difference between the p13 number that was measured on six-jet data (91%) and the average value coming from our trigger parametrization (87%).
- The uncertainty from the SVT tag probabilities. These are listed in table V.

systematic uncertainties on signal efficiency (in %)		
Vertex reconstruction	$\pm 1$	
Jet Identification	-9.8	-
Jet Energy Scale $\pm\sigma$	-28.3	+28.1
Jet Resolution $\pm\sigma$	-0.6	+0.2
Top Mass $\pm 5\text{GeV}/c^2$	-7.6	+5.9
Trigger Efficiency(trigsim)	$\pm 4$	

TABLE IV: Systematic error calculation on signal efficiency.

- The uncertainty on the background parametrization. As was elaborately discussed in section , there is an error on the background parametrization we use. We include this error in the systematical uncertainty.
- The uncertainty of the background parametrization due to limited statistics. We take the maximal error from the different  $H_T$  bins, which is 3.6% when  $450 < H_T < 100$  GeV.

We observe that the error is currently completely dominated by the Jet Energy Scale, Top Mass measurement and background estimation. The total combined systematic error on the measurement is

$$\text{syst change on } \epsilon = +32.3\% - 32.2\%.$$

The individual and combined systematic error can be seen in figure 34.

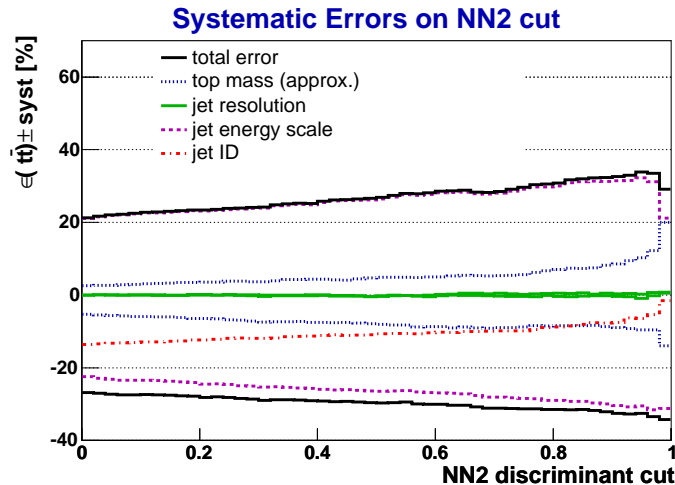


FIG. 34: Systematic errors on the efficiency as a function of the NN2 cut.

## VIII. CONCLUSION

We have measured the top and anti-top quark ( $\bar{t}t$ ) pair cross section in the top to 'all-jets' channel using an event sample corresponding approximately  $162 \text{ pb}^{-1}$ , which was recorded by DØ in the period 2002/2003.

<b>systematic uncertainties on tagging probabilities (in %)</b>		
Taggability		$\pm 0.6$
Taggability flavor dependence		$\pm 0.0$
SLT efficiency (data)	-3.7	2.9
SLT efficiency (MC)		$\pm 0.5$
inclusive $b$ -efficiency (MC)		$\pm 0.2$
inclusive $c$ -efficiency (MC)		$< 10^{-3}$
Scale Factor $b/c$	-0.1	0.0
negative tag efficiency		$\pm 0.1$
$M_{top} \pm 5$ GeV	-0.2	+0.4
Limited MC statistics		$\pm 1.1$

TABLE V: *Systematic uncertainties from SVT modeling.*

<b>systematic uncertainties on background estimation (in %)</b>	
Statistical error TRFs	$\pm 3.6$
Background modeling (TRFs)	$\pm 6.6$
Total	$\pm 7.5$

TABLE VI: *Systematic error calculation on background calculation.*

The analysis is restricted to events with at least six jets (and no isolated lepton); the expected signature for  $t\bar{t}$  pairs decaying in a  $b$  quark and a  $W$  boson and the subsequent decay of each  $W$  boson into 2 quarks.

The background from QCD events is reduced using several variables related to the topology and the underlying physical structure of the events. These variables are combined in a chain of two artificial neural networks, after which we apply a secondary vertex tag (SVT) to reduce background. The efficiency after a cut on the output on the second neural network is

$$\epsilon \cdot \text{BR} = 0.0273 \pm 0.0009(\text{stat})_{-0.0079}^{+0.0086}(\text{syst}) \quad (10)$$

The remaining background is predicted using all events except events with a double tag, weighted with event weights predicted by a SVT tag rate function. We observe 220 events, where we predict  $186 \pm 5(\text{stat}) \pm 12(\text{syst})$  background events. Presuming a  $t\bar{t}$  cross section of  $7 \text{ pb}^{-1}$ , we would expect 28 signal events. The measured cross section is

$$\sigma(t\bar{t}) = 7.7 \pm 3.5(\text{stat})_{-1.9}^{+3.7}(\text{syst}) \pm 0.5(\text{lumi}) \text{ pb.}$$

## IX. ACKNOWLEDGEMENTS

We would like to thank the Top Production group, and in particular Lisa Shabalina and Aurelio Juste for their fruitful discussions and input on the analysis.

---

[1] *F. Blekman and M. Vreeswijk, Measurement of the  $t\bar{t} \rightarrow$  hadrons production cross section using p14 data*, DØ note 4333, March 2004.

- [2] *F. Blekman and M. Vreeswijk*, **Measurement of the  $t\bar{t} \rightarrow$  hadrons production cross section using p13 data**, DØ note 4175, July 2003.
- [3] *R. Schwienhorst* **Top Trigger Selection and Application of Turn On Curves to the Monte Carlo**, [http://www-d0.fnal.gov/Run2Physics/top/d0\\_private/wg/triggers/Note\\_Reinhard\\_Jan2004.pdf](http://www-d0.fnal.gov/Run2Physics/top/d0_private/wg/triggers/Note_Reinhard_Jan2004.pdf), January 2004.
- [4] *The Top Physics Working Group of the DØ Collaboration*, **DØ Top Analysis and Data Sample for the Winter Conferences 2004**, DØ note XXXX, [http://www-d0.fnal.gov/Run2Physics/top/private/winter04/winter04\\_top\\_note\\_v0\\_3.ps](http://www-d0.fnal.gov/Run2Physics/top/private/winter04/winter04_top_note_v0_3.ps)
- [5] *R. Demina, T. Golling, A. Juste, A. Khanov, F. Rizatdinova, E. Shabalina, J. Strandberg*, **Measurement of the  $t\bar{t} \rightarrow$  hadrons production cross section at  $\sqrt{s} = 1.96$  TeV using lifetime tagging**, DØ note 41415, July 2003.
- [6] *C. Peterson, T. Rognvaldsson and L. Lonnblad*, **JETNET 3.0: A Versatile artificial neural network package**, *Comput. Phys. Commun.* **81**, 185 (1994).